J. Fluid Mech. (1965), *vol.* 21, *part* 2, *pp.* 257–280
Printed in Great Britain

A non-linear theory for symmetric, supercavitating flow in a gravity field

By CHARLES W. LENAU
University of Missouri
AND ROBERT L. STREET
Stanford University

(Received 6 February 1964 and in revised form 24 June 1964)

An analysis is made of the effect of a longitudinal gravity field on two-dimensional supercavitating flow past wedges. Under the assumption that the flow is both irrotational and incompressible, a non-linear theory is developed for steady flow. By utilizing conformal mapping in combination with the Schwarz reflexion principle, the mathematical problem is reduced to a three-parameter, non-linear integral equation with one constraint. The equation is derived by reflecting the flow about the rigid boundaries; the constraint is obtained by requiring the net singularity strength inside the cavity-wedge system to be zero. A successive-approximation procedure is used to obtain a numerical solution of the integral equation. Typical results are presented in graphs and tables, and the results of the present work are compared to those of Acosta's linear theory.

1. Introduction

A considerable number of models and analyses have been created to describe the cavity flows that occur in the underwater operation of high-speed submarines, missiles, and hydrofoil structures. These analyses, almost all of which are based on two-dimensional, incompressible, ideal-fluid flow, have in general neglected the effect of gravity and surface tension. According to Gilbarg (1960), comparison of widely contrasting cavity models with water-tunnel measurements indicates that the usual assumptions of free-streamline theory and experiment agree for drag and cavity dimensions. Gilbarg also notes that the influence of gravity on drag is not clear, but that distortion of cavities due to buoyancy is often apparent. Because supercavitation is likely to occur, in water, in the same speed range for both large and small bodies, smaller Froude numbers can be expected with larger bodies. Thus, while gravity may have little effect on the drag or cavity dimensions of small bodies, such as those used in water-tunnel experiments, the effects of gravity may be important for larger bodies.

Attempts to include gravity in the analysis of cavity flows have been infrequent due in major part to the complexity of the solution. In linearized analyses, the effects of gravity have been successfully included by Parkin (1957), Acosta (1961), and Street (1963). The solutions obtained by Parkin and Street applied to transverse gravity fields and contained approximations in addition to those of the linearization. Acosta's solution for a longitudinal gravity field is exact within the framework of linearized theory. In general, however, one is usually forced to deal with some sort of approximate solution which is laborious in nature, or to seek an exact solution by an inverse method in order to solve any problem which has a free surface in a gravity field. New hope has been found, however, for the approximate solution in the development of high-speed digital computers upon which, indeed, the present work relies.

In cavity-flow analyses, it is assumed that the pressure in the cavity is constant and the flow field pressure is everywhere greater than the cavity pressure. These conditions are satisfied approximately by actual supercavitating flows. Since cavitation occurs locally in a fluid field when pressure drops to the vapour pressure, the latter condition insures that no cavitation will occur outside the cavity zone. For the gravity-free case these conditions become:

(1) The speed on the cavity streamline is constant.

(2) The maximum flow field speed occurs on the cavity streamline.

Condition 2 implies that the cavity is convex as viewed from the fluid field. Conditions 1 and 2 present a difficulty if the cavity is to close. Condition 1 excludes closure with a stagnation point and condition 2 excludes a cusp. When gravity is considered, the situation is more complex. First, it may be possible to close a cavity with a stagnation point without violating the constant-pressure condition. Furthermore, it is conceivable that a portion of the cavity-free streamline can be concave; thus cusps are not excluded. However, for a flow model to be valid over a range of Froude numbers, including infinity, a cusp or stagnation point cannot be used for closure.

The present work deals with a symmetric wedge of arbitrary included angle and cavity with gravity acting parallel to the axis of symmetry. The flow model, originally used by Geurst (1961) for gravity-free flow, employs a flat plate mounted normal to the stream to close the cavity. This model is presumed to yield approximately the drag coefficient and cavity dimensions for actual cavity flow about a wedge which is rising or descending at constant velocity in an infinite fluid at rest, or for the flow of an infinite stream past a stationary wedge with gravity acting parallel to the stream.

2. Problem definition

The wedge and cavity are shown in figure 1. The co-ordinate system is fixed to the wedge in order to obtain a steady-state flow field with the origin at the vertex of the wedge. Gravity is considered positive when it acts in the positive x-direction. It is assumed that the velocity components (u, v) are bounded, continuous functions of space and that as $z \to \infty$, $(u, v) \to (U_\infty, 0)$; and furthermore, that only two stagnation points occur in the flow field, one at the vertex of the wedge and the other at the centre of the closure plate. It is assumed that the cavity and wedge form a body symmetric about the x-axis and finally, that the flow is steady and irrotational and the fluid is incompressible and inviscid.

It is well known that for any two-dimensional, steady-state, irrotational flow of incompressible, inviscid fluid there exists a complex potential $W = \phi + i\psi$ whose real and imaginary parts are the potential ϕ and stream function ψ. Moreover, $W(z)$ will be analytic at each point, not on a boundary, at which the velocity components $u = \partial\phi/\partial x$ and $v = \partial\phi/\partial y$ are continuous. Furthermore, the complex velocity $dW/dz = u - iv$ is analytic at each point where $W(z)$ is analytic.

The mathematical problem is formulated in terms of analytic function theory. Let D be the domain consisting of the lower half plane minus the cavity and

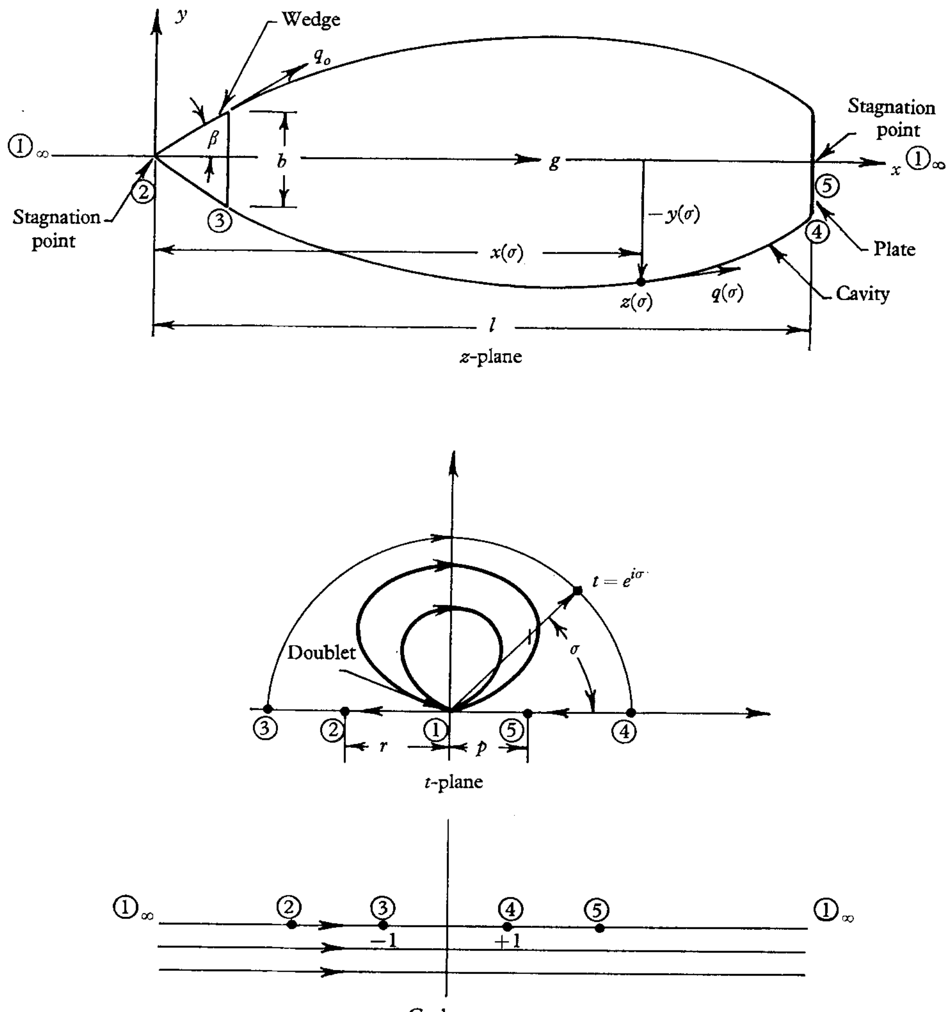

FIGURE 1. Physical and auxiliary planes.

wedge so that the boundary $\bar{D}$ coincides with the lower branch of the split streamline. Let D^* be the domain formed by the reflexion of D about the x-axis into the upper half plane. It is evident, then, that:

(1) For $z \in D \cup D^*$, dW/dz is analytic and single-valued;

(2) For $z \in \bar{D} \cup \bar{D}^*$, dW/dz is bounded and continuous;

(3) For $z \in D \cup \bar{D} \cup D^* \cup \bar{D}^*$, dW/dz vanishes only at points (2) and (5);

(4) Gravity acts parallel to the x-axis;

(5) As $z \to \infty$, $dW/dz \to U_\infty$;

(6) The cavity and wedge form a body symmetric about the x-axis.

The above statements follow from the preceding assumptions. As a result of the continuity of the velocity components (u, v), $W(z)$ and dW/dz are analytic for $z \in D \cup D^*$, and the complex velocity dW/dz must be single-valued for $z \in D \cup D^*$ because the velocity components are single-valued.

From the above conditions it can be shown that for a given Froude number

$$F^2 = q_0^2/gb, \tag{1}$$

and cavitation number

$$\Sigma = \frac{P_\infty - P_K}{\frac{1}{2}\rho U_\infty^2} = \left(\frac{q_0}{U_\infty}\right)^2 - 1, \tag{2}$$

one and only one solution exists, provided only that the Froude number is sufficiently large. The term q_0 is the speed in the velocity field at the point of detachment, g is the acceleration of gravity, and b is the base width of the wedge. The term P_K is the cavity pressure, ρ is the density of the fluid, and P_∞ and U_∞ are the pressure and velocity in the stream at a point far from the wedge but at the same x-elevation as the separation points.

The method used in this work is closely related to that used in Birkhoff & Carter's (1957) treatment of rising plane bubbles and de Boor's (1961) treatment of the sluice gate, and the latter method in turn has many similarities to the Levi–Civita method (Birkhoff & Zarantonello 1957 and Milne-Thompson 1961) for treating cavity models with curved bodies.

The symmetry of the present problem allows the solution to be simplified by replacing the streamline from points (1) to (2) and (5) to (1) by a fixed boundary and considering only the lower half plane. Thus, the flow field is contained in the simply connected domain D.

As in most (if not all) non-linear solutions to two-dimensional problems with free boundaries, the central role is played by

$$\zeta = \frac{1}{q_0}\frac{dW}{dz} = \frac{1}{q_0}(u - iv).$$

A convenient domain Γ in an auxiliary t-plane is introduced where the complex potential $W(z)$ and the complex velocity $\zeta(z)$ are found as functions of t. The above expression may then be written

$$\zeta[z(t)] = \frac{1}{q_0}\frac{dW}{dt}[z(t)]\frac{dt}{dz},$$

and the t and z planes are related by the transformation

$$z = \frac{1}{q_0}\int \frac{1}{\zeta[z(t)]}\frac{dW}{dt}[z(t)]\,dt.$$

The choice of Γ is made to simplify the solution as much as possible; indeed, this choice allows the fixed boundary to be removed from discussion. The domain Γ is the semicircle $|t| < 1$, $\operatorname{Im}\{t\} > 0$. The free streamline corresponds to the arc of the semicircle, and the fixed boundary to its diameter, such that the point at infinity corresponds to the origin (figure 1). The mapping function $z = f(t)$ which maps Γ on to D will be analytic, single-valued, and univalent for

$t \in \Gamma$ and continuous for $t \in \overline{\Gamma}$, $t \neq 0$, where $\overline{\Gamma}$ is the boundary of Γ. The constants, $0 < r; p < 1$ depend on the geometry of the physical plane and are functions of Σ and F^2.

The approach used is to replace the complex velocity by

$$\zeta(t) = \mu(t)\, e^{\Omega(t)},$$

where $\mu(t)$ is a known function and $\Omega(t)$ is an unknown function which is analytic in $|t| < 1$ and real valued for $-1 < t < 1$. The function $\mu(t)$ is selected so that $\Omega(t)$ satisfies these conditions. The two properties of $\Omega(t)$ allow it to be represented by a power series with real coefficients, which converges for $|t| < 1$. Since the coefficients are unknown, the power series is truncated to form a polynomial with a finite set of unknown coefficients. These coefficients are then found by satisfying approximately the constant-pressure condition on the free streamline. The solution of the problem will allow computation of the basic physical parameters F^2, l/b, C_D, and Σ in terms of two independent non-physical parameters Λ^* and r, that are defined later.

3. Formulation of the integral equation

From the definition of the auxiliary domain Γ and the character of the physical and the complex potential planes, it is possible to establish the functions

$$W = W(t),$$

and

$$\zeta = \zeta(t) = \mu(t)\, e^{\Omega(t)}.$$

It is shown in appendix 1 that

$$W(t) = K\left(t + \frac{1}{t}\right), \tag{3}$$

i.e. the singularity is a doublet in a circle with an unknown strength K, and

$$\zeta(t) = e^{-\frac{1}{2}\pi i}\left(\frac{r+t}{1+rt}\right)^{\beta/\pi}\left(\frac{t-p}{1-pt}\right)^{\frac{1}{2}} e^{\Omega(t)}. \tag{4}$$

For $t = e^{i\sigma}$, $0 \leqslant \sigma \leqslant \pi$, $\zeta(t)$ will be the conjugate of the free-streamline velocity. For the gravity-free case, $|\zeta(e^{i\sigma})| = 1$, hence, equation (4) becomes

$$|\zeta(e^{i\sigma})| = \left|\frac{r+e^{i\sigma}}{1+r\,e^{i\sigma}}\right|^{\beta/\pi}\left|\frac{e^{i\sigma}-p}{1-p\,e^{i\sigma}}\right|^{\frac{1}{2}} \exp\left[\operatorname{Re}\{\Omega(e^{i\sigma})\}\right] = \exp\left[\operatorname{Re}\{\Omega(e^{i\sigma})\}\right]$$

or

$$\operatorname{Re}\{\Omega(e^{i\sigma})\} = 0, \quad \operatorname{Im}\{i\Omega(e^{i\sigma})\} = 0.$$

Moreover, since $\Omega(e^{i\sigma}) = \overline{\Omega(e^{-i\sigma})}$ for $0 \leqslant \sigma \leqslant \pi$, then $\operatorname{Im}\{i\Omega(e^{i\sigma})\} = 0$ for $0 \leqslant \sigma < 2\pi$. The function $i\Omega(t)$ is analytic in $|t| < 1$, continuous and real-valued for $|t| = 1$. By the reflexion principle, $i\Omega(t)$ will be analytic in the entire plane including the point at infinity. Hence, by the Liouville theorem, $i\Omega(t)$ must be a constant, and $\Omega(t) = ic$, where c is a real number. But as $t \to 0$, $\zeta(t) \to U_\infty/q_0$; hence, $c = 0$. Consequently,

$$\zeta(t) = e^{-\frac{1}{2}\pi i}\left(\frac{r+t}{1+rt}\right)^{\beta/\pi}\left(\frac{t-p}{1-tp}\right)^{\frac{1}{2}}$$

for the gravity-free case.

The free streamline in the physical plane corresponds to $t = e^{i\sigma}$, $0 \leqslant \sigma \leqslant \pi$ in the t plane. Combining the definitions

$$\left.\begin{aligned} \phi(\sigma)+i\epsilon(\sigma) &= \Omega(e^{i\sigma}), \quad \theta(\sigma) = \cos^{-1}\left[\frac{-2p+\cos\sigma(1+p^2)}{1-2p\cos\sigma+p^2}\right], \\ \psi(\sigma) &= \cos^{-1}\left[\frac{2r+\cos\sigma(1+r^2)}{1+2r\cos\sigma+r^2}\right], \quad \Delta(\sigma) = \tfrac{1}{2}\theta(\sigma)+\beta/\pi\psi(\sigma) \end{aligned}\right\} \tag{5}$$

with equation (4) produces

$$\zeta(e^{i\sigma}) = \exp\left[-\tfrac{1}{2}\pi i + i\Delta(\sigma) + i\epsilon(\sigma) + \phi(\sigma)\right]. \tag{6}$$

Substituting $t = e^{i\sigma}$ into equation (3) gives

$$W = 2K\cos\sigma.$$

Combining this relationship with

$$\zeta = \frac{1}{q_0}\frac{dW}{d\sigma}\frac{d\sigma}{dz}$$

and equation (6) gives

$$\frac{dz(\sigma)}{d\sigma} = -\frac{2K}{q_0}\sin\sigma\exp\left(\tfrac{1}{2}\pi i - \Delta i - \epsilon i - \phi\right),$$

where $z(\sigma)$ locates a point on the free streamline. The integrated equation is

$$z(\sigma) = \frac{b\,e^{-i\beta}}{2\sin\beta} + \frac{2K}{q_0}\int_\sigma^\pi \sin\xi\exp\left[\left(\tfrac{1}{2}\pi - \Delta - \epsilon\right)i - \phi\right]d\xi$$

and clearly,

$$x(\sigma) = \tfrac{1}{2}b\cot\beta + \frac{2K}{q_0}\int_\sigma^\pi \sin\xi\sin(\Delta+\epsilon)\,e^{-\phi}\,d\xi, \tag{7}$$

$$y(\sigma) = -\tfrac{1}{2}b + \frac{2K}{q_0}\int_\sigma^\pi \sin\xi\cos(\Delta+\epsilon)\,e^{-\phi}\,d\xi. \tag{8}$$

The speed $q(\sigma)$ at a point on the free streamline is easily found from equation (6) by using

$$(q/q_0)^2 = \zeta\bar{\zeta} \tag{9}$$

to achieve

$$(q/q_0)^2 = e^{2\phi}. \tag{10}$$

For the pressure to be constant along the free streamline, the proper relationship between $x(\sigma)$ and $q(\sigma)$, given by Bernoulli's equation, must be satisfied. Writing the Bernoulli equation between (3) and the arbitrary point $z(\sigma)$ on the free streamline and assuming gravity to act in the positive x-direction gives, after some rearranging,

$$1 + \frac{2g}{q_0^2}\left[x(\sigma) - \tfrac{1}{2}b\cot\beta\right] = \left(\frac{q}{q_0}\right)^2.$$

Combining (7) and (10) with the above expression yields

$$e^{2\phi} = 1 + \frac{4gK}{q_0^3}\int_\sigma^\pi \sin\xi\sin(\Delta+\epsilon)\,e^{-\phi}\,d\xi. \tag{11}$$

If the functions ϕ and ϵ can be determined from the above equation, the function $\Omega(t)$ will be completely defined since its values on the boundary $|t| = 1$ will be known. Proof of the existence and uniqueness of this solution is given in Lenau (1963).

4. Relations between the flow parameters and the drag coefficient

From (2) and (4) with $t = 0$

$$\Sigma = \frac{e^{-2\Omega(0)}}{pr^{2\beta/\pi}} - 1. \tag{12}$$

The parameters p and r are related by requiring the cavity to be closed. Expanding the complex velocity into a power series about the point at infinity in the z-plane gives

$$\zeta(z) = U_\infty + \frac{\alpha_1}{z} + \frac{\alpha_2}{z^2} + \dots, \quad |z| > R. \tag{13}$$

The coefficients are real since $\zeta(z)$ is real-valued for real values of z. Evaluating the integral

$$\oint_c \zeta(a)\, dz$$

along a closed contour c which encloses the circle $|z| = R$ gives

$$\oint_c \zeta(z)\, dz = 2\pi i \alpha_1.$$

The imaginary part of the above integral is proportional to the net flux of fluid flowing out of the contour c (Parkin 1959). Since $\zeta(z)$ has no singularities exterior to the cavity and wedge system (by hypothesis), setting $\alpha_1 = 0$ constitutes a necessary and sufficient condition for cavity closure. Substituting equation (A. 1.2) (appendix 1) into (13) produces

$$\zeta(t) = U_\infty + \frac{\alpha_1}{\beta_{-1}} t + \left(\frac{\alpha_2}{\beta_{-1}} - \frac{\alpha_1 \beta_0}{\beta_{-1}}\right) t^2 + \dots$$

and the closure condition becomes

$$\zeta'(0) = 0.$$

Performing this operation on equation (4) gives

$$\Omega'(0) - \frac{1}{2}\left(\frac{1-p^2}{p}\right) + \frac{\beta}{\pi}\left(\frac{1-r^2}{r}\right) = 0.$$

Solving this equation for p gives

$$p = -\Omega'(0) - \frac{\beta}{\pi}\left(\frac{1-r^2}{r}\right) \pm \left\{1 + \left[\Omega'(0) + \frac{\beta}{\pi}\left(\frac{1-r^2}{r}\right)\right]^2\right\}^{\frac{1}{2}}.$$

The constant p locates the point (5) in the t-plane and $0 < p < 1$. Hence, the above equation has meaning only if

$$p = -\Omega'(0) - \frac{\beta}{\pi}\left(\frac{1-r^2}{r}\right) + \left\{1 + \left[\Omega'(0) + \frac{\beta}{\pi}\left(\frac{1-r^2}{r}\right)\right]^2\right\}^{\frac{1}{2}}, \tag{14}$$

and

$$\Omega'(0) > -\frac{\beta}{\pi}\left(\frac{1-r^2}{r}\right).$$

The physical meaning of this inequality and the limitation imposed by it upon the solution are discussed later.

If the substitution $t = -\xi$ is made, equation (4) becomes for $-1 < t < -r$

$$\zeta(\xi) = e^{i\beta}\left(\frac{\xi - r}{1-\xi r}\right)^{\beta/\pi}\left(\frac{p+\xi}{1+p\xi}\right)^{\frac{1}{2}} e^{\Omega(-\xi)}. \tag{15}$$

Furthermore,

$$\frac{dW}{d\xi} = K\left(\frac{1}{\xi^2}-1\right)$$

and

$$\zeta = \frac{K}{q_0}\left(\frac{1}{\xi^2}-1\right)\frac{d\xi}{dz}.$$

Solving for $dz/d\xi$ and using (15) produces

$$\frac{dz}{d\xi} = \frac{K}{q_0}\left(\frac{1}{\xi^2}-1\right)e^{-i\beta}\left(\frac{1-r\xi}{\xi-r}\right)^{\beta/\pi}\left(\frac{1+p\xi}{p+\xi}\right)^{\frac{1}{2}} e^{-\Omega(-\xi)}. \tag{16}$$

Integrating between points (2) and (3) gives

$$z_3 - z_2 = \frac{K\,e^{-i\beta}}{q_0}\int_r^1 \left(\frac{1}{\xi^2}-1\right)\left(\frac{1-r\xi}{\xi-r}\right)^{\beta/\pi}\left(\frac{1+\xi p}{p+\xi}\right)^{\frac{1}{2}} e^{-\Omega(-\xi)}\,d\xi.$$

Since $|z_3 - z_2| = \frac{1}{2}b\csc\beta$,

$$K = (bq_0/2I_1)\csc\beta \tag{17}$$

where

$$I_1 = \int_r^1 \left(\frac{1}{\xi^2}-1\right)\left(\frac{1-r\xi}{\xi-r}\right)^{\beta/\pi}\left(\frac{1+\xi p}{p+\xi}\right)^{\frac{1}{2}} e^{-\Omega(-\xi)}\,d\xi, \tag{18}$$

The drag force D, found by integrating $(P-P_k)$ over the face of the wedge, is

$$D = \int_0^{\frac{1}{2}b\csc\beta} (P-P_k)\,ds\,2\sin\beta.$$

Writing the Bernoulli equation from the point s on the wedge face to the separation point, solving for $(P-P_k)$, and combining the above results with (1) gives

$$D = \rho q_0^2 \sin\beta \int_0^{\frac{1}{2}b\csc\beta}\left[1-\left(\frac{q}{q_0}\right)^2 - \frac{1}{F^2}\left(\frac{1}{\sin\beta}-\frac{2s}{b}\cot\beta\right)\right]ds.$$

Performing in part the integration yields

$$D = -\rho q_0^2 \sin\beta \int_0^{\frac{1}{2}b\csc\beta}\left(\frac{q}{q_0}\right)^2 ds + \rho\frac{q_0^2 b}{2}\left(1-\frac{\cot\beta}{2F^2}\right). \tag{19}$$

Combining (9) and (15) gives

$$\left(\frac{q}{q_0}\right)^2 = \left(\frac{\xi-r}{1-r\xi}\right)^{2\beta/\pi}\left(\frac{p+\xi}{1+p\xi}\right)e^{2\Omega(-\xi)}.$$

From (16),

$$\frac{ds}{d\xi} = \frac{K}{q_0}\left(\frac{1}{\xi^2}-1\right)\left(\frac{1-r\xi}{\xi-r}\right)^{\beta/\pi}\left(\frac{1+\xi p}{p+\xi}\right)^{\frac{1}{2}} e^{-\Omega(-\xi)};$$

therefore

$$\int_0^{\frac{1}{2}b\csc\beta}\left(\frac{q}{q_0}\right)^2 ds = \frac{K}{q_0}\int_r^1\left(\frac{1}{\xi^2}-1\right)\left(\frac{\xi-r}{1-r\xi}\right)^{\beta/\pi}\left(\frac{p+\xi}{1+p\xi}\right)^{\frac{1}{2}} e^{\Omega(-\xi)}\,d\xi.$$

If $$I_2 = \int_r^1 \left(\frac{1}{\xi^2}-1\right)\left(\frac{\xi-r}{1-r\xi}\right)^{\beta/\pi}\left(\frac{p+\xi}{1+p\xi}\right)^{\frac{1}{2}} e^{\Omega(-\xi)}\,d\xi, \tag{20}$$

equation (19) may be written as

$$D = \rho\frac{q_0^2 b}{2}\left(1-\frac{\cot\beta}{2F^2}-\frac{2KI_2}{bq_0}\sin\beta\right).$$

Combining the above results with (2) and (17) and with the definition

$$C_D = D/\tfrac{1}{2}\rho U_\infty^2 b$$

produces $$C_D = (1+\Sigma)\left(1-\frac{I_2}{I_1}-\frac{\cot\beta}{2F^2}\right). \tag{21}$$

5. Solution of the integral equation

It has been shown previously that $\Omega(t)$ is a continuous function of t for $|t| = 1$. Hence, the real and imaginary parts of $\Omega(e^{i\sigma})$ will be continuous functions of σ. Equation (11) shows, however, that if $\phi(\sigma)$ and $\epsilon(\sigma)$ are continuous functions of σ, the right side of the integral equation will have a continuous derivative, which implies that $\phi(\sigma)$ has a continuous derivative. The methods used herein to construct solutions to the above integral equation can yield solutions only of this class.

The function $\Omega(t)$ is analytic for $|t| < 1$ and real-valued for $-1 < t < 1$. Hence, it may be expanded into a power series about the origin as

$$\Omega(t) = a_0 + a_1 t + a_2 t^2 + \dots.$$

The coefficients are real numbers since $\Omega(t)$ is real-valued for real values of t. For $t = e^{i\sigma}$

$$\phi(\sigma)+i\epsilon(\sigma) = \sum_{\nu=0}^{\infty} a_\nu \cos\nu\sigma + i\sum_{\nu=1}^{\infty} a_\nu \sin\nu\sigma$$

or $$\phi(\sigma) = \sum_{\nu=0}^{\infty} a_\nu \cos\nu\sigma, \quad \epsilon(\sigma) = \sum_{\nu=1}^{\infty} a_\nu \sin\nu\sigma.$$

Since $\phi'(\sigma)$ is continuous, $\sum_{\nu=0}^{\infty} a_\nu \cos\nu\sigma$ will converge uniformly. Moreover, $\sum_{\nu=1}^{\infty} a_\nu \sin\nu\sigma$ will also converge uniformly, as is shown in Lenau (1963).

The integral equation in terms of these expansions becomes

$$\exp\left(2\sum_{\nu=0}^{\infty} a_\nu \cos\nu\sigma\right) = 1+\frac{4qK}{q_0^3}\int_\sigma^\pi \sin\xi \sin\left(\Delta+\sum_{\nu=1}^{\infty} a_\nu \sin\nu\xi\right)\exp\left(-\sum_{\nu=0}^{\infty} a_\nu\cos\nu\xi\right)d\xi.$$

Differentiating the above equation and rearranging slightly leads to

$$\sum_{\nu=1}^{\infty} \nu a_\nu \sin\nu\sigma = \frac{2gK\,e^{-3a_0}}{q_0^3}\sin\sigma\sin\left(\Delta+\sum_{\nu=1}^{\infty} a_\nu\sin\nu\xi\right)\exp\left(-3\sum_{\nu=1}^{\infty} a_\nu\cos\nu\xi\right). \tag{22}$$

Solving for the Fourier coefficient on the left side of the above equation gives

$$na_n = \frac{\Lambda}{3}\int_0^\pi \sin\sigma \sin\left(\Delta + \sum_{\nu=1}^{\infty} a_\nu \sin\nu\sigma\right)\exp\left(-3\sum_{\nu=1}^{\infty} a_\nu \cos\nu\sigma\right)\sin n\sigma\, d\sigma, \quad (23)$$

where

$$\Lambda = 12gKe^{-3a_0}/\pi q_0^3. \quad (24)$$

Equation (22) may also be written

$$\frac{d}{d\sigma}\left[\exp\left(3\sum_{\nu=1}^{\infty} a_\nu \cos\nu\sigma\right)\right] = \frac{-6gKe^{-3a_0}}{\pi q_0^3}\sin\sigma\sin\left(\Delta + \sum_{\nu=1}^{\infty} a_\nu \sin\nu\sigma\right).$$

If

$$\exp\left(3\sum_{\nu=1}^{\infty} a_\nu \cos\nu\sigma\right) = \sum_{\nu=1}^{\infty} C_\nu \cos\nu\sigma, \quad (25)$$

the above equation becomes

$$\sum_{\nu=1}^{\infty} \nu C_\nu \sin\nu\sigma = \frac{6gKe^{-3a_0}}{q_0^3}\sin\sigma\sin\left(\Delta + \sum_{\nu=1}^{\infty} a_\nu \sin\nu\sigma\right).$$

Solving for Fourier coefficient C_n and combining with (24) gives

$$nC_n = \Lambda\int_0^\pi \sin\sigma\sin\left(\Delta + \sum_{\nu=1}^{\infty} a_\nu \sin\nu\sigma\right)\sin n\sigma\, d\sigma. \quad (26)$$

Replacing $\Omega'(0)$ by a_1 in (14) produces

$$p = -a_1 - \frac{\beta}{\pi}\left(\frac{1-r^2}{r}\right) + \left\{1 + \left[a_1 + \frac{\beta}{\pi}\left(\frac{1-r^2}{r}\right)\right]^2\right\}^{\frac{1}{2}}.$$

Two successive-approximation procedures have been devised and used to construct solutions to (11). The first, the simpler of the two, converges slowly and has been used only to check the results obtained by the second procedure. The second method is more complicated and difficult to use but appears to converge rapidly for almost all cases of physical significance. In both methods Λ and r are independent parameters.

Method I

For the first successive-approximation procedure, (23) is replaced by the recursion formula

$$a_j^{k+1} = \frac{\Lambda}{3j}\int_0^\pi \sin\sigma\sin\left(\Delta^k + \sum_{\nu=1}^{N} a_\nu^k \sin\nu\sigma\right)\exp\left(-3\sum_{\nu=1}^{N} a_\nu\cos\nu\sigma\right)\sin(j\sigma)\, d\sigma$$

$$(j = 1, 2, 3, \ldots, N)$$

where from (5)

$$\Delta^k = \tfrac{1}{2}\cos^{-1}\left\{\frac{-2p^k + \cos\sigma[1+(p^k)^2]}{1 - 2p^k\cos\sigma + (p^k)^2}\right\} + \frac{\beta}{\pi}\cos^{-1}\left\{\frac{2r + \cos\sigma(1+r^2)}{1 + 2r\cos\sigma + r^2}\right\}$$

and

$$p^k = -a_1^k - \frac{\beta}{\pi}\left(\frac{1-r^2}{r}\right) + \left\{1 + \left[a_1^k + \frac{\beta}{\pi}\left(\frac{1-r^2}{r}\right)\right]^2\right\}^{\frac{1}{2}}.$$

The superscript k denotes the kth approximation of the quantity in question. This procedure is initiated by setting $a_j^0 = 0$ for $j = 1, 2, 3, \ldots, N$ and assigning values to the parameters Λ and r. This procedure is continued until the desired accuracy is obtained.

Method II

For this method (26) is replaced by the recursion formula

$$C_j^{k+1} = \frac{\Lambda}{j}\int_0^\pi \sin\sigma \sin\left(\Delta^k + \sum_{\nu=1}^{N} a_\nu^k \sin \nu\sigma\right)\sin(j\sigma)\,d\sigma \quad (j = 1, 2, 3, \ldots, N), \quad (27)$$

and (23) is replaced by the following systems of equations (see appendix 2)

$$\left.\begin{aligned}
e_0^k &= 1,\\
\tfrac{1}{2}C_1^k &= e_0^k e_1^k + e_1^k e_2^k + e_2^k e_3^k + \ldots + e_{N-1}^k e_N^k,\\
\tfrac{1}{2}C_2^k &= e_0^k e_2^k + e_1^k e_3^k + e_2^k e_4^k + \ldots + e_{N-2}^k e_N^k,\\
&\cdots\cdots\cdots\cdots\cdots\cdots\cdots\cdots\\
\tfrac{1}{2}C_j^k &= e_0^k e_j^k + \ldots + e_i^k e_{i+j}^k + \ldots + e_{N-j}^k e_N^k,\\
&\cdots\cdots\cdots\cdots\cdots\cdots\cdots\cdots\\
\tfrac{1}{2}C_{N-1}^k &= e_0^k e_{N-1}^k + e_1^k e_N^k,\\
\tfrac{1}{2}C_N^k &= e_0^k e_N^k
\end{aligned}\right\} \quad (28)$$

and

$$\left.\begin{aligned}
e_0^k &= 1,\\
e_1^k &= e_0^k b_1^k,\\
2e_2^k &= 2e_0^k b_2^k + e_1^k b_1^k,\\
3e_3^k &= 3e_0^k b_3^k + 2e_1^k b_2^k + e_2^k b_1^k,\\
&\cdots\cdots\cdots\cdots\cdots\cdots\cdots\cdots\\
je_j^k &= je_0^k b_j^k + (j-1)\,e_1^k b_{j-1}^k + \ldots + (j-i)\,e_i^k b_{j-i}^k + \ldots e_{j-1}^k b_1^k,\\
&\cdots\cdots\cdots\cdots\cdots\cdots\cdots\cdots\\
Ne_N^k &= Ne_0^k b_N^k + (N-1)\,e_1^k b_{N-1}^k + \ldots + e_{N-1}^k b_1^k,
\end{aligned}\right\} \quad (29)$$

and $$a_j^k = \tfrac{2}{3}b_j^k \quad \text{for} \quad j = 1, 2, 3, \ldots, N.$$

This procedure is initiated, just as in the first method, by setting $a_j^0 = 0$ for $j = 1, 2, 3, \ldots, N$ and assigning values to Λ and r. This allows the set $\{C_j^1\}$ to be evaluated, which in turn allows the sets $\{e_j^1\}$, $\{b_j^1\}$, and $\{a_j^1\}$ to be evaluated. The set $\{a_j^1\}$ is used to evaluate set $\{C_j^2\}$ and the process is repeated.

The non-linear system of equations defined by (28) is solved by a relaxation technique. Residues are defined for the first $(N-1)$ equations such that

$$F_j = \tfrac{1}{2}C_j^k - e_0^k e_j^k - e_1^k e_{j+1}^k - \ldots - e_{N-j}^k e_N^k \quad (j = 1, 2, 3, \ldots, N-1).$$

Derivatives are found to be

$$\partial F_j/\partial e_i^k = -e_{i-j}^k - e_{i+j}^k \quad \text{if} \quad e_j^k = 0 \quad \text{for} \quad j < 0 \quad \text{and} \quad j > n.$$

The relaxation procedure is initiated by setting $e_i^k = 0$ for $i = 1, 2, 3, \ldots, N-1$, $e_0^k = 1$ and $e_N^k = \frac{1}{2}C_N^k$. The maximum residue $|F_\nu|$ is selected and Δe_ν^k found from

$$F_\nu + \Delta e_\nu^k(\partial F_\nu/\partial e_\nu^k) = 0.$$

Each residue F_i is then replaced by $F_i + \Delta e_\nu^k(\partial F_i/\partial e_\nu^k)$. Lastly, e_ν^k is replaced by $e_\nu^k + \Delta e_\nu^k$ and the maximum residue is again selected and the process is repeated.

It is convenient to introduce a new independent parameter Λ^* which is related to Λ and r by the equation

$$\Lambda^* = \Lambda \int_0^\pi \sin^2\sigma \sin\Delta\, d\sigma. \tag{30}$$

It is seen from (27) that

$$\Lambda^* = C_1^0,$$

i.e. Λ^* is the first approximation to the coefficient C_1. This parameter essentially determines the ratio q_e/q_0 where q_e is the free streamline speed at the end of the cavity. In fact

$$q_e/q_0 \approx \exp(\tfrac{2}{3}\Lambda^*).$$

This simple relationship derived in Lenau (1963) is based on the observation that in most cases of interest:

(1) The coefficients c_1^k and a_1^k change very little with k;

(2) The coefficients c_1^k and a_1^k dominate the higher-order terms in their respective series.

The procedure for obtaining numerical results is now described. Values of r and Λ^* are assigned; Λ is determined from (30), and the integral equation is solved by one of the successive-approximation procedures. This determines p and a_ν for $\nu = 1, 2, 3, \ldots, N$. The lead coefficient a_0 can now be determined since it is easily shown from the above that

$$a_0 = a_1 - a_2 + a_3 + \ldots (-1)^{N+1} a_N. \tag{31}$$

Thus

$$\Omega(t) = \sum_{\nu=0}^{N} a_\nu t^\nu$$

is now completely defined; hence, I_1 and I_2 may be evaluated using (18) and (20). The Froude number is computed by combining (17) and (24). Cavity dimensions may be determined by combining (17), (7), and (8). Finally, Σ may be determined from (12), and the drag coefficients from (21).

All numerical integrations have been accomplished by dividing the interval of integration into J even divisions giving J subintervals. The integration was then carried out over each subinterval according to the Gauss quadrature formula for four divisions (Scarborough 1955). The number of subintervals used depended upon the definite integral being evaluated. Those defined in (27) were evaluated using 10 subintervals if 10 coefficients a_j were to be determined, and 15 subintervals for 15 coefficients. The definite integrals contained in (18) and (20) were evaluated using 15 subintervals. However, since the integrand in (18) is singular and therefore unsuited for numerical quadrature, the singularity is first removed by integrating by parts.

The condition of constant pressure on the free streamline is not satisfied exactly by the obtained solutions. Hence, a check must be made on the cavity streamline speed to see how closely the Bernoulli equation is satisfied. The quantity chosen for this measure is

$$\tau(\sigma) = [q^2_{x(\sigma)} - q^2(\sigma)]/q^2_{x(\sigma)},$$

where $q(\sigma)$ is the speed that actually occurs on the cavity streamline at elevation $x(\sigma)$, and $q_{x(\sigma)}$ is the speed that should occur here. Writing the Bernoulli equation from the separation point to $z(\sigma)$ gives

$$1+\frac{2g}{q_0^2}(x(\sigma)-\tfrac{1}{2}b\cot\beta) = \left(\frac{q_{x(\sigma)}}{q_0}\right)^2.$$

Hence,
$$\tau(\sigma) = 1-\left(\frac{q_{(\sigma)}}{q_0}\right)^2\left\{1+\frac{2g}{q_0^2}\,[x(\sigma)-\tfrac{1}{2}b\cot\beta]\right\}^{-1}.$$

Combining the above expressions with (7), (10), and (24) gives

$$\tau(\sigma) = 1-\frac{\exp\left(2\sum\limits_{\nu=0}^{N} a_\nu\cos\nu\sigma\right)}{1+\dfrac{e^{3a_0}\Lambda\pi}{3}\displaystyle\int_\sigma^\pi \sin\xi\sin\left(\Delta+\sum_{\nu=1}^{N} a_\nu\sin\nu\xi\right)\exp\left(-\sum_{\nu=0}^{N} a_\nu\cos\nu\xi\right)d\xi}.$$

6. Results and discussion

Both successive-approximation procedures were used to construct solutions to the integral equation. Method II was in all cases a superior procedure, for it converged more rapidly than method I and for a greater range of Λ^*. Table 1 contains the successive approximations to the coefficients $\{a_j\}$ obtained by both methods for $\Lambda^* = 0{\cdot}75$ and $r = 0{\cdot}57$. For method I seven iterations were needed to stabilize the lead coefficient a_1 to within 0·04 % of its apparent ultimate value. For method II four iterations stabilized the lead coefficient to within 0·004 % of the same value. In general, it has been found that the number of iterations necessary to stabilize the coefficients depends essentially on $|\Lambda^*|$, with the number of iterations increasing with $|\Lambda^*|$ until the procedure fails to converge. For example, for $\Lambda^* = 2{\cdot}0$ and $r = 0{\cdot}55$ method I diverges, while for method II the lead coefficient stabilized to within 0·03 % of its final value after eight iterations.

Figure 2 is a plot of $\tau(\sigma)$ *vs* σ for various values of Λ^* using the coefficients obtained by method II. It is seen that the quantity

$$\|\tau\| \equiv \max_{0\leqslant\sigma\leqslant\pi} |\tau(\sigma)|$$

increases with Λ^*. For 10 coefficients and $\Lambda^* < 1{\cdot}0$, $\|\tau\|$ is less than 0·03 % but for Λ^* in excess of 1·0, $\|\tau\|$ increases rapidly—reaching a value of about 10 % for $\Lambda^* = 2{\cdot}0$. This increase in $\|\tau\|$ with Λ^* is apparent in the coefficients obtained. For $\Lambda^* = 1{\cdot}0$ the size of the coefficients decreases rapidly, the ratio of the tenth to the first being about 0·0005. For $\Lambda^* = 2{\cdot}0$ the first six coefficients are almost equal in size and the ratio of the tenth to the first coefficient is about 0·02. For 15 coefficients the behaviour of $\|\tau\|$ is similar to, but its magnitude is smaller than, that obtained with 10 coefficients. For $\Lambda^* = 2{\cdot}0$, $\|\tau\|$ is about one-half that obtained by using 10 coefficients. Table 2 contains the computed values of $1/F^2$, Σ, c_0 and l/b using 10 and 15 coefficients. For $\Lambda^* = 2{\cdot}0$ these quantities change by less than 2 %. For $\Lambda^* = 1{\cdot}5$ a change of less than 0·6 % is obtained. For $\Lambda^* = 1{\cdot}0$ these differences have been reduced to less than 0·07 %. It has been found in general that if $|\Lambda^*| \leqslant 1$ and 10 coefficients are used, then $\|\tau\| < 0{\cdot}5\,\%$. It has also been found that in almost all cases $|\Lambda^*|$ in excess of 1·0 has no physical significance. For these reasons 10 coefficients have been used for all computations presented in this work. Based on the above and similar results, it appears that these computations are within 0·5 % of their correct values.

a_1	a_2	a_3	a_4	a_5
		Method I		
0·250000	−0·000262	−0·000430	−0·000163	−0·000192
0·264300	−0·048737	0·004890	−0·001177	−0·000345
0·247039	−0·050316	0·011250	−0·003750	0·000339
0·243561	−0·045405	0·010128	−0·003990	0·000616
0·245026	−0·044906	0·009355	−0·003630	0·000519
0·245468	−0·045373	0·009425	−0·003578	0·000476
0·245346	−0·045452	0·009508	−0·003613	0·000483
a_6	a_7	a_8	a_9	a_{10}
−0·000106	−0·000108	−0·000072	−0·000069	−0·000051
−0·000218	−0·000170	−0·000098	−0·000080	−0·000047
−0·000427	−0·000135	−0·000120	−0·000080	−0·000053
−0·000576	−0·000078	−0·000148	−0·000075	−0·000060
−0·000556	−0·000077	−0·000150	−0·000073	−0·000060
−0·000535	−0·000085	−0·000147	−0·000074	−0·000060
−0·000535	−0·000086	−0·000146	−0·000074	−0·000060
		Method II		
a_1	a_2	a_3	a_4	a_5
0·250043	−0·047006	0·011376	−0·003268	0·000814
0·245164	−0·045313	0·009439	−0·003611	0·000487
0·245312	−0·045406	0·009500	−0·003617	0·000487
0·254307	−0·045403	0·009498	−0·003617	0·000487
a_6	a_7	a_8	a_9	a_{10}
−0·000317	0·000014	−0·000054	−0·000031	−0·000039
−0·000542	−0·000082	−0·000152	−0·000063	−0·000088
−0·000538	−0·000083	−0·000150	−0·000064	−0·000088
−0·000538	−0·000083	−0·000150	−0·000064	−0·000088

TABLE 1. Successive approximations to the set $\{a_j\}$ of series coefficients obtained by using method I and method II for $r = 0{\cdot}57$, $\Lambda^* = 0{\cdot}75$

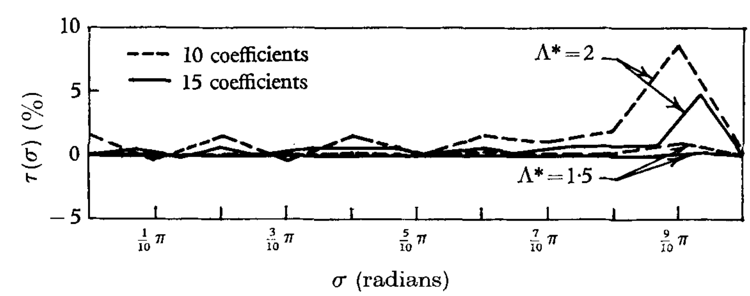

FIGURE 2. Pressure error function: $\tau(\sigma)$ *vs* σ for $\beta = 15°$; $r = 0{\cdot}55$.

It has been shown that the cavity closure condition relates r, p, and a_1, that $0 < p < 1$, and that for this to be true,

$$a_1 > -\frac{\beta}{\pi}\left(\frac{1-r^2}{r}\right).$$

Since $0 < r < 1$, no difficulty will occur when $a_1 > 0$. However, negative values of a_1 occur with negative values of Λ^*. For a given r, Λ^* may be decreased until

$$a_1 = -\frac{\beta}{\pi}\left(\frac{1-r^2}{r}\right).$$

When this occurs $p = 1$ and the closure plate has vanished. Moreover, equation (10) shows that the free-streamline velocity at the end of the cavity has not vanished. Examination of equation (4) reveals that the singularity

$$[(p-t)(1-pt)]^{\frac{1}{2}}$$

has vanished and a stagnation point no longer occurs at the end of the cavity. Plots of such cavities reveal that the cavity is terminated by a cusp. As p approaches 1 the closure plate decreases in size and the end of the cavity becomes pointed. For $p = 0{\cdot}999$ the cavity shape is almost identical to the cusped cavity although it still has a stagnation point at the end of the cavity. Figures 3 and 4 give two examples of cavity shapes for p close to 1. Examples of cusped cavities may be found in figures 5 and 6. For a given value of r, a value of Λ^* may be found which gives a cusped cavity. This value represents the greatest lower bound of Λ^* for which a solution exists to the Geurst model. If Λ^* is decreased beyond this point, the integral equation still has a solution but a value of p greater than unity will be obtained. Lenau (1963) gives the solution to the problem of a cusped-cavity model.

r	Λ^*	N	Σ	C_D	$1/F^2$	l/b
0·55	2·00	10	−0·8098	−0·7921	1·6278	9·580
0·55	2·00	15	−0·8234	−0·8053	1·7562	9·559
0·55	1·50	10	−0·5948	−0·4404	0·4320	11·691
0·55	1·50	15	−0·5973	−0·4428	0·4347	11·689
0·55	1·00	10	−0·3028	−0·1088	0·1239	14·109
0·55	1·00	15	−0·3027	−0·1087	0·1239	14·109
0·55	0·50	10	−0·0115	0·1683	0·0322	16·631
0·55	0·50	15	−0·0114	0·1684	0·0322	16·631

TABLE 2. Examples of various parameters when $\beta = 15°$, $r = 0{\cdot}55$

Figures 7 to 13 illustrate the dependence of l/b and C_D on Σ and F. The plots of l/b *vs* Σ (figures 7–10) reveal that l/b is greatly affected by F. Figure 14 shows a number of cavities for $\Sigma = 0{\cdot}28$. It is seen that positive F^2 tend to reduce l/b and to increase the size of the closure plate. Conversely, negative F^2 tend to increase l/b and to decrease the size of the closure plate, the limiting case being the cusped cavity. For a given negative F^2, Σ decreases with increasing l/b until a minimum value occurs at the cusped cavity. The effect of F^2 on C_D is illustrated by figures 11 and 13. Positive F^2 decrease C_D, and negative F^2 increase it. This

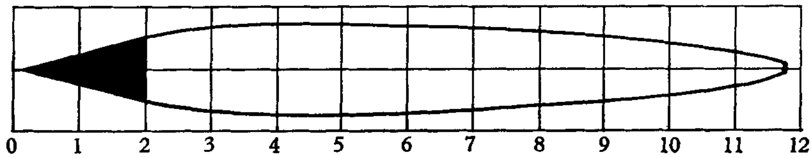

FIGURE 3. Cavity shape: $\beta = 15°$; $p = 0{\cdot}922$.

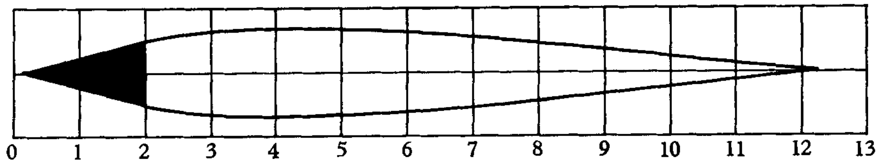

FIGURE 4. Cavity shape: $\beta = 15°$; $p = 0{\cdot}980$.

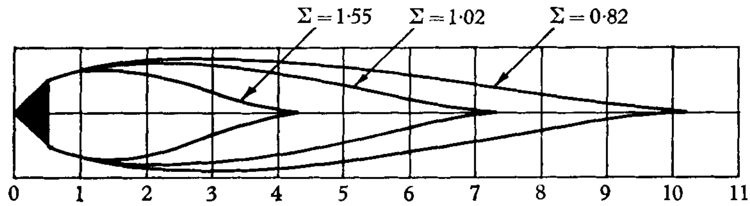

FIGURE 5. Cavity shapes for cusped cavities: $\beta = 45°$.

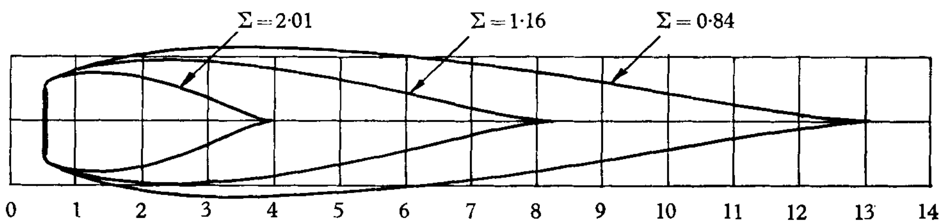

FIGURE 6. Cavity shapes for cusped cavities: $\beta = 90°$.

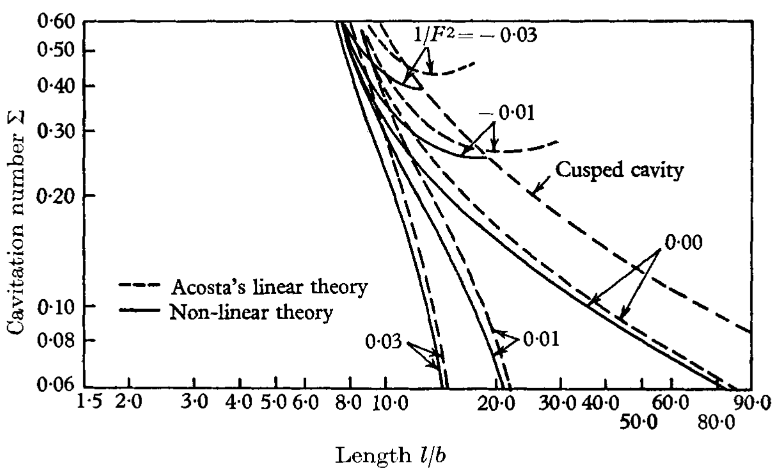

FIGURE 7. A comparison between the cavitation numbers obtained from Acosta's linear theory and those obtained from the non-linear theory for a range of cavity lengths for $\beta = 5°$.

is consistent with the direction of the buoyancy force. For negative F^2 the buoyancy force is in the direction of flow, and conversely, for positive F^2 the buoyancy force is opposite to the direction of flow. The effect that a given F^2 has

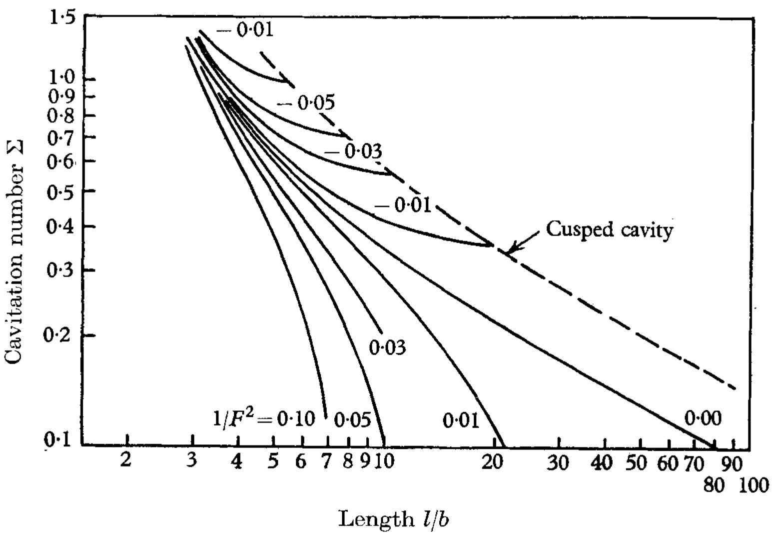

FIGURE 8. Cavitation number *vs* length for $\beta = 15°$.

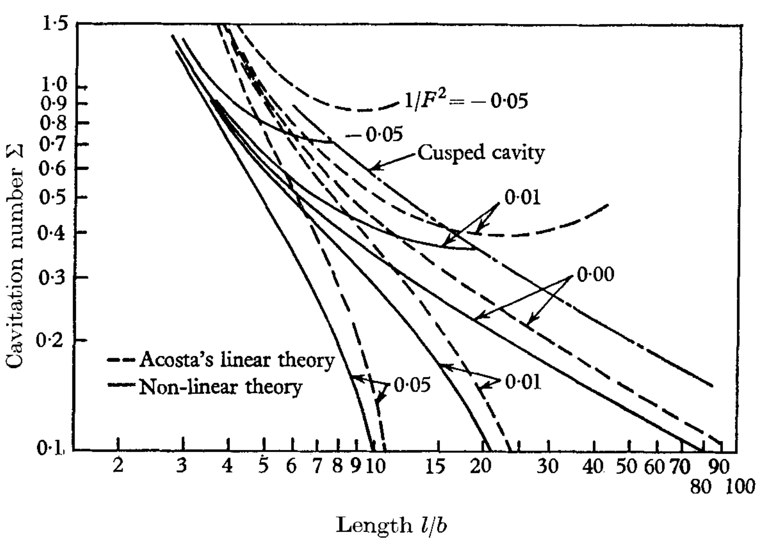

FIGURE 9. A comparison between the cavitation numbers obtained from Acosta's linear theory and those obtained from the non-linear theory for a range of cavity lengths for $\beta = 15°$.

on C_D increases with decreasing wedge angles. For a wedge half angle of 45° the curves $1/F^2 = \pm 0{\cdot}01$ almost coincide with the gravity-free case. For a wedge half angle of 5° the curves $1/F^2 = \pm 0{\cdot}01$ are substantially displaced from the $1/F^2 = 0$ case.

Figures 7, 9, 11, and 12 compare the results of Acosta's linear theory and the present work. For a wedge half angle of 5°, agreement between l/b and C_D for the two theories is good for small Σ. It is not expected that the two theories

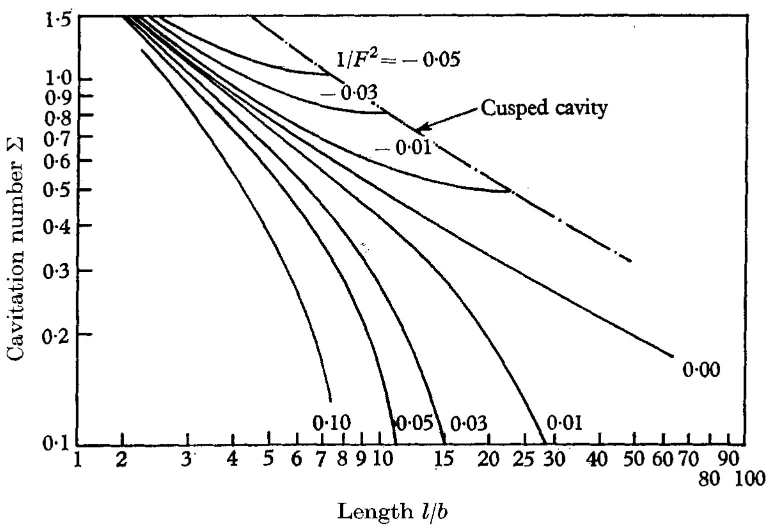

FIGURE 10. Cavitation number *vs* length for $\beta = 45°$.

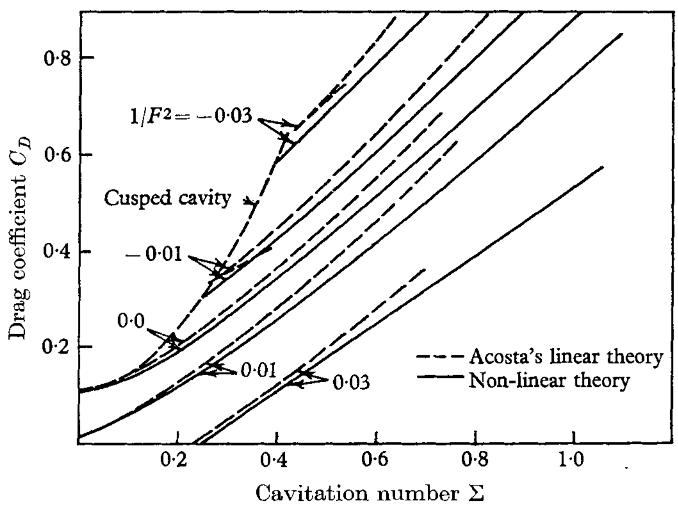

FIGURE 11. A comparison between the drag coefficients obtained from Acosta's linear theory and those obtained from the non-linear theory for a range of the cavitation number for $\beta = 5°$.

should agree elsewhere since first-order Σ are a basic assumption of linear theories. For a wedge angle of 15° the quantitative agreement is poor but the curves do agree qualitatively.

In Lenau (1963) it is shown that for a given r and Λ, a solution to the Geurst-model problem exists and is unique provided $|\Lambda|$ is sufficiently small. However,

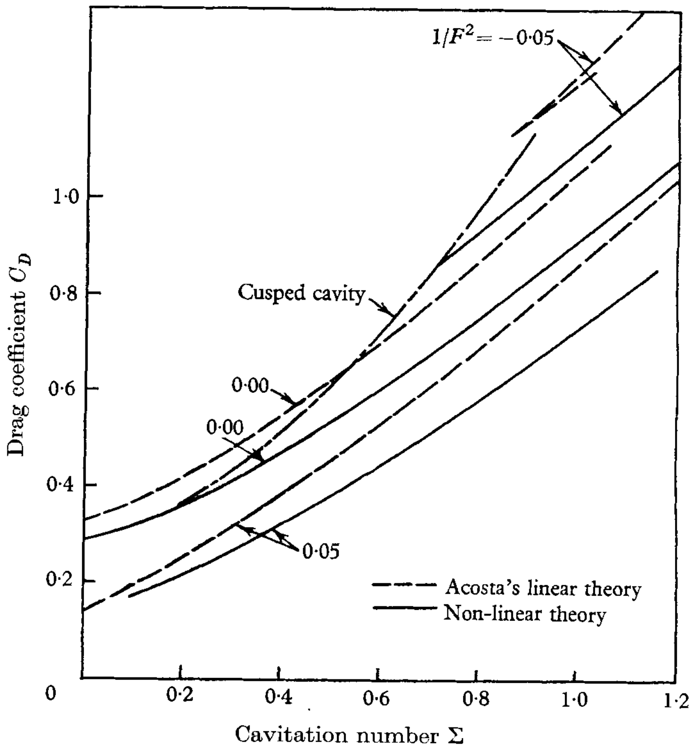

FIGURE 12. A comparison between the drag coefficients obtained from Acosta's linear theory and those obtained from the non-linear theory for a range of cavitation numbers for $\beta = 15°$.

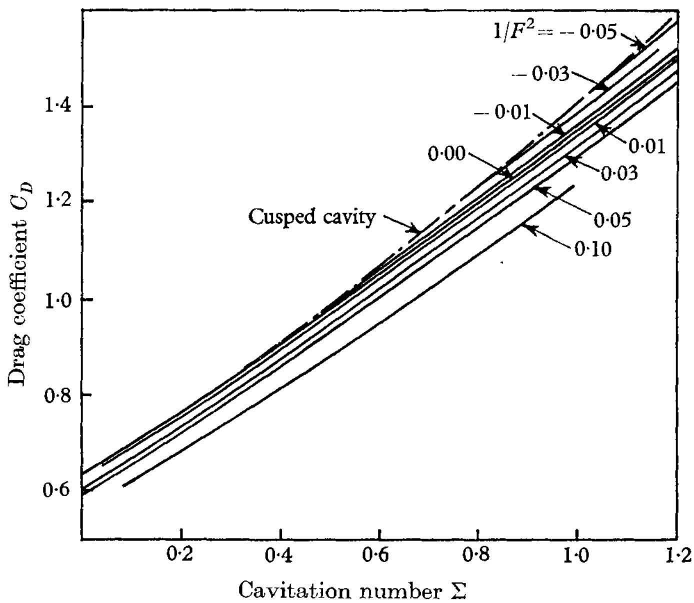

FIGURE 13. Drag coefficient *vs* cavitation number for $\beta = 45°$.

it has not been established that for a given F and Σ there will be a unique solution. Indeed, non-uniqueness is expected since Acosta's linear theory gives, in many cases, two solutions for each F^2 and Σ. These solutions may be seen by examining figures 7 and 9. For a given negative F^2, Σ decreases with increasing l/b until

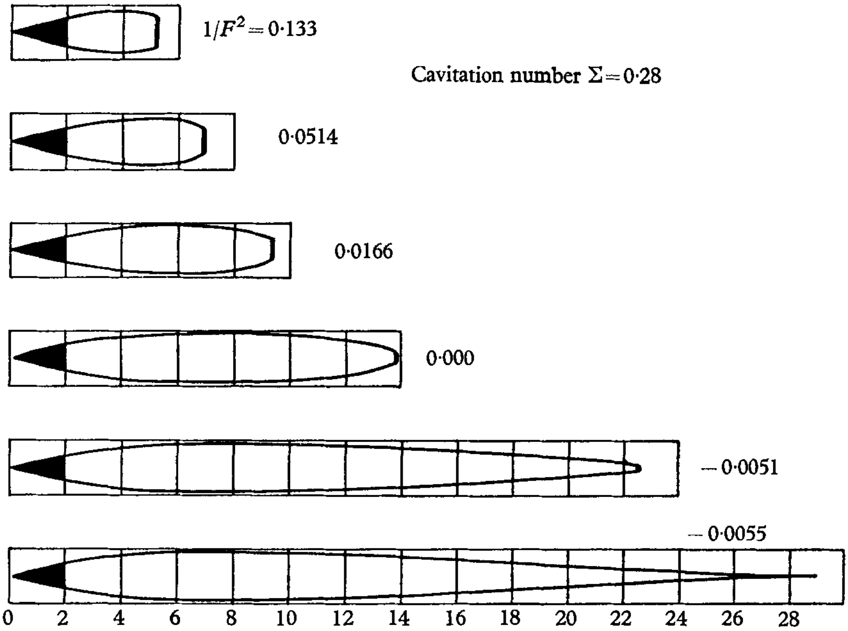

FIGURE 14. Cavity shapes at constant cavitation number for $\beta = 15°$.

a minimum Σ is reached. Beyond this point Σ increases with l/b giving a second length for each Σ. Two drag coefficients also occur for each cavitation number, as shown in figures 11 and 12. The Geurst model has given no indication of this behaviour. It appears from the plots of Σ *vs* l/b (figures 7–10) that for a given negative F^2 the minimum Σ occurs at the cusped cavity. Indeed, the slopes of these curves appear to be zero at this point.

Appendix 1

In this appendix we develop the required functions $W = W(t)$ and $\zeta = \zeta(t)$. Recall that the domain D consists of the lower half of the z-plane minus the cavity and wedge while the domain Γ is the semicircle $|t| < 1$, $\mathrm{Im}\{t\} > 0$.

Based on the hypotheses made earlier about $\zeta(z)$, it is shown subsequently that the mapping function $f(t) = z$, which maps the domain Γ onto D, exists and is continuous for $t \in \overline{\Gamma}$, $t \neq 0$. The complex potential $W(z)$ will be analytic for $z \in D$ and continuous for $z \in \overline{D}$. The transformation $T = W(z)$ maps the domain D onto the lower half of the T plane with the point at infinity going into the point at infinity. The function $W(z)$ is univalent; hence, it has an inverse $W^{-1}(T) = z$ which is continuous for real values of T. A linear transformation of the form

$$T = 2GK + B$$

will map the lower half of the T plane on to the lower half of the G plane, the point at infinity mapping into the point at infinity. The choice of the appropriate constants K and B causes points (3) and (4) to map into -1 and 1, respectively. The function $G = \frac{1}{2}[t+t^{-1}]$ maps Γ onto the lower half of the G plane such that points $1, 0, -1$ map into points $1, \infty, -1$ respectively. Hence,

$$z = W^{-1}[K(t+t^{-1})+B]$$

which is continuous for $t \in \overline{\Gamma}$, $t \neq 0$, maps Γ on to D in the same manner as $f(t)$. According to the fundamental theorems of conformal mapping, this function must be unique; hence, $f(t) = W^{-1}[K(t+t^{-1})+B]$, thus establishing that $f(t)$ is continuous for $t \in \overline{\Gamma}$, $t \neq 0$. Moreover,

$$W[f(t)] = [K(t+t^{-1})+B].$$

Setting $B = 0$ and denoting $W[f(t)]$ by $W(t)$ in the above equation produces

$$W(t) = K(t+t^{-1}). \tag{A. 1.1}$$

The singularity then is a doublet in a circle with an unknown strength K.

It is instructive to examine the function $1/f(t)$ in the domain $|t| < \delta$, $0 < \delta < \min(r, p)$. This function is analytic for $|t| < \delta$, $\operatorname{Im}\{t\} > 0$ and continuous and real-valued for $-\delta < t < \delta$ (taking the value zero at $t = 0$). Thus, it follows from the Schwarz reflexion principle (Nehari 1952) that $1/f(t)$ is analytic for $|t| < \delta$. Moreover, $1/f(t)$ has a non-vanishing derivative at $t = 0$ because it maps conformally at this point. If $1/f(t)$ is expanded into a power series about zero, then

$$1/f(t) = t(\alpha_1+\alpha_2 t+\alpha_3 t^2+\ldots) \quad (\alpha_1 \neq 0).$$

It is seen that $f(t)$ has a simple pole at $t = 0$ and may be written

$$f(t) = \beta_{-1}/t+\beta_0+\beta_1 t+\ldots, \tag{A. 1.2}$$

where the coefficients are real.

A knowledge of the singularities of $z = f(t)$ at $t = p$ and $t = -r$ is necessary in order to determine the singularities of $\zeta(t)$ at these points. The singularity can be determined for the point $t = -r$ by considering $f(t)$ in the domain

$$\Delta\colon \{|t+r| < \delta, \operatorname{Im}\{t\} > 0\}, 0 < \delta < \min(r, 1-r).$$

The image domain in the z-plane will have as a part of its boundary two straight-line segments which intersect at $z = 0$ and correspond to $-\delta < t+r < \delta$ in the t-plane. Hence,

$$h(t) = (e^{\pi i}z)^{1/[1-(\beta/\pi)]} = [e^{\pi i}f(t)]^{1/[1-(\beta/\pi)]}$$

will be analytic for $t \in \Delta$ and continuous and real-valued for $-\delta < r+t < \delta$ (Nehari 1952). Thus, by the reflexion principle $h(t)$ is analytic in $|t+r| < \delta$. Moreover, $h(t)$ possesses a non-vanishing derivative at $t = -r$ since it maps conformally here. After $h(t)$ is expanded into a power series about the point $t = -r$

$$h(t) = [e^{\pi i}f(t)]^{1/[1-(\beta/\pi)]} = (t+r)[\gamma_1+\gamma_2(t+r)+\gamma_3(t+r)^2\ldots] \quad (\gamma_1 \neq 0).$$

The above equation may be solved for $f(t)$, producing

$$f(t) = e^{-\pi i}(t+r)^{1-\beta/\pi}\left[\sum_{\nu=1}^{\infty}\gamma_\nu(t+r)^{\nu-1}\right]^{1-\beta/\pi} = e^{-\pi i}(t+r)^{1-\beta/\pi}F_1(t).$$

Since $\sum_{\nu=1}^{\infty} \gamma_\nu (t+r)^{\nu-1}$ does not vanish at $t = -r$, $F_1(t)$ will be analytic at this point. Differentiating the above expression and collecting terms yields

$$f'(t) = e^{-\pi i} F_2(t)/(t+r)^{\beta/\pi}, \tag{A. 1.3}$$

where $$F_2(t) = [F_1'(t)\,(t+r) + (1-\beta/\pi)\,F_1(t)].$$

The function $F_2(t)$ will be analytic and non-vanishing for $t = -r$ provided $\beta/\pi < 1$. By a similar argument $f'(t)$ is found to be

$$f'(t) = e^{-\pi i} F_3(t)/(t-p)^{\frac{1}{2}}, \tag{A. 1.4}$$

where $F_3(t)$ is analytic and non-vanishing at $t = p$.

The function $\omega(t) = \log\{\zeta[f(t)]\}$ will be analytic for $t \in \Gamma$ and continuous for $t \in \overline{\Gamma}$ except at the stagnation points where $\zeta[f(t)]$ vanishes. The nature of these singularities is determined by combining (A. 1.1), (A. 1.3), and (A. 1.4) with

$$\zeta[f(t)] \equiv \zeta(t) = \frac{1}{q_0}\frac{W'(t)}{f'(t)}.$$

Hence, near $t = -r$, $\omega(t) = (\beta/\pi)\log(t+r) + F_5(t)$

and near $t = p$, $\omega(t) = \frac{1}{2}\log(t-p) + F_6(t)$ (A. 1.5)

where $$F_5(t) = \log\left[\frac{K}{q_0}\left(1-\frac{1}{t^2}\right)\right] - \log F_2(t) + \pi i,$$

and $$F_6(t) = \log\left[\frac{K}{q_0}\left(1-\frac{1}{t^2}\right)\right] - \log F_3(t) + \pi i$$

are analytic at the point in question because $F_2(t)$ and $F_3(t)$ are analytic and non-vanishing here. From an examination of $\omega(t)$ for real values to t, it follows that

$$\left.\begin{aligned} \operatorname{Im}\{\omega(t)\} &= -\tfrac{1}{2}\pi \quad (p < t < 1),\\ \operatorname{Im}\{\omega(t)\} &= 0 \quad (-r < t < p),\\ \operatorname{Im}\{\omega(t)\} &= \beta \quad (-1 < t < -r).\end{aligned}\right\} \tag{A. 1.6}$$

In view of (A. 1.5)

$$\Omega(t) = \omega(t) - (\beta/\pi)\log(r+t) - \tfrac{1}{2}\log(t-p) + \tfrac{1}{2}\pi i + (\beta/\pi)\log(1+rt) + \tfrac{1}{2}\log(1-pt) \tag{A. 1.7}$$

is analytic for $t \in \Gamma$ and continuous for $t \in \overline{\Gamma}$. The choice of the proper branches of the logarithm functions in combination with (A. 1.5) produces

$$\begin{aligned} \operatorname{Im}\{\Omega(t)\} &= -\tfrac{1}{2}\pi + \tfrac{1}{2}\pi = 0 \quad (p < t < 1),\\ \operatorname{Im}\{\Omega(t)\} &= -\tfrac{1}{2}\pi + \tfrac{1}{2}\pi = 0 \quad (-r < t < p),\\ \operatorname{Im}\{\Omega(t)\} &= \beta - \beta = 0 \quad (-1 < t < -r).\end{aligned}$$

By the Schwarz reflexion principle, $\Omega(t)$, which is real-valued for $-1 < t < 1$, may be continued analytically across the real axis into the reflexion of Γ. Hence, $\Omega(t)$ is analytic in $|t| < 1$ and continuous in $|t| = 1$. Rearranging (A. 1.7) and using

$$\zeta(t) = e^{\omega(t)}$$

produces $$\zeta(t) = e^{-\frac{1}{2}\pi i}\left(\frac{r+t}{1+rt}\right)^{\beta/\pi}\left(\frac{t-p}{1-pt}\right)^{\frac{1}{2}} e^{\Omega(t)}. \tag{A. 1.8}$$

Appendix 2

In this Appendix we derive the equation sets (28) and (29) that are used in numerical method II. These sets, which relate the coefficient sets $\{C_j^k\}\{a_j^k\}$, evolve from the relationship

$$\exp\left(\sum_{\nu=1}^{\infty} b_\nu t^\nu\right) = \sum_{\nu=0}^{\infty} e_\nu t^\nu = U(t). \tag{A. 2.1}$$

The coefficient set $\{b_\nu\}$ is related to the coefficient set $\{e_\nu\}$ by Taylor's formula, i.e.

$$e_N = U^{(N)}(0)/N!. \tag{A. 2.2}$$

Derivatives of $U(t)$ are given by (Dwight 1961)

$$U^{(k+1)}(t) = \sum_{i=0}^{k} U^{(i)}(t)\, g^{(k-i)}(t)\, \frac{k!}{(k-i)!\,i!},$$

where
$$g(t) = \sum_{\nu=1}^{\infty} \nu b_\nu t^{\nu-1}.$$

Combining this relationship with the above expression and setting $t = 0$ gives

$$U^{(k+1)}(0) = \sum_{i=0}^{k} \frac{U^{(i)}(0)\, g^{(k-i)}(0)\, k!}{(k-i)!\,i!} \tag{A. 1.3}$$

where
$$g^{(k)}(0) = b_{k+1}(k+1)!.$$

Combining this expression with (A. 1.2) and (A. 2.3) produces

$$(k+1)\, e_{k+1} = \sum_{i=0}^{k} e_i b_{k-i+1}(k-i+1) \quad \text{for} \quad k = 0, 1, 2, 3, \ldots.$$

Clearly, $e_0 = U(0) = 1$. Substituting $t = e^{i\sigma}$ in (A. 2. 1) gives

$$U(e^{i\sigma}) = \sum_{\nu=0}^{\infty} e_\nu e^{i\nu\sigma} = \exp\left(\sum_{\nu=1}^{\infty} b_\nu e^{i\nu\sigma}\right).$$

Forming the product $U(e^{i\sigma})\, U(e^{-i\sigma})$ produces

$$\exp\left(2\sum_{\nu=1}^{\infty} b_\nu \cos \nu\sigma\right) = (e_0^2+e_1^2+e_2^2+\ldots)+2(e_0e_1+e_1e_2+e_2e_3+\ldots)\cos\sigma$$
$$+2(e_0e_2+e_1e_3+e_2e_4+\ldots)\cos 2\sigma+\ldots+2(e_0e_n+e_1e_{n+1}+\ldots)\cos n\sigma+\ldots.$$

Hence, by setting

$$2b_\nu = 3a_\nu \quad \text{for} \quad \nu = 1, 2, 3, \ldots$$

and
$$C_\nu = 2\sum_{i=0}^{\infty} e_i e_{\nu+1}$$

a relationship between $\{e_\nu\}$ and $\{a_\nu\}$ is established. In summary these equations are

$$C_j = 2\sum_{i=0}^{\infty} e_i e_{i+j} \quad \text{for} \quad j = 1, 2, 3, \ldots,$$
$$e_0 = 1,$$
$$(j+1)e_{j+1} = \sum_{i=0}^{j} e_i b_{j-i+1}(j-i+1) \quad \text{for} \quad j = 0, 1, 2, \ldots,$$
$$2b_j = 3a_j \quad \text{for} \quad j = 1, 2, 3, \ldots.$$

Adding superscripts and truncating these infinite series at N terms gives (28) and (29). It is clear that (25) is satisfied exactly only for $N = \infty$.

The authors express their sincere appreciation to Stanford Profs Byrne Perry, who first suggested this investigation, and Gordon Latta, who contributed to the mathematical rigour of the work through many helpful discussions. The research was carried out at Stanford University under the Bureau of Ships Fundamental Hydromechanics Research Program, and National Science Foundation Grant No. NSF-GP 948 provided support for the numerical computations. Reproduction in whole or in part is permitted for any purpose of the United States Government.

REFERENCES

ACOSTA, A. J. 1961 The effect of a longitudinal gravity field on the supercavitating flow over a wedge. *J. Appl. Mech.* **28**; *Trans. ASME*, 83, Series E, pp. 188–92.

BIRKHOFF, G. & CARTER, D. 1957 Rising plane bubbles. *J. Rat. Mech. Anal.* **6**, 6.

BIRKHOFF, G. & ZARANTONELLO, E. 1957 *Jets, Wakes, and Cavities.* New York: Academic Press.

DE BOOR, C. 1961 Flow under a sluice gate. Report under Nonr-1866(34), Harvard University, Cambridge, Mass.

DWIGHT, H. B. 1961 *Tables of Integrals and Other Mathematical Data*, 4th ed. New York: Macmillan.

GEURST, J. A. 1961 Linearized theory of two-dimensional cavity flows. Doc. diss., Technische Hogeschool Te Delft.

GILBARG, D. 1960 Jets and cavities, vol. IX, *Encyclopedia of Physics.* Berlin: Springer-Verlag.

LENAU, C. W. 1963 A nonlinear theory for supercavitating flow past a wedge in a longitudinal gravity field. *Dept. of C.E. Tech. Rep.* no. 28, Stanford University, Stanford, Calif.

MILNE-THOMPSON, L. M. 1961 *Theoretical Hydrodynamics*, 4th ed. New York: Macmillan.

NEHARI, Z. 1952 *Conformal Mapping.* New York: McGraw-Hill.

PARKIN, B. R. 1957 A note on the cavity flow past a hydrofoil in a liquid with gravity. *Engr. Div. Tech. Rep.* no. 47–9, CIT, Pasadena, Calif.

PARKIN, B. R. 1959 Linearized theory of cavity flow in two dimensions. *RAND Corp. Rep.* no. P 1745, Santa Monica, Calif.

SCARBOROUGH, J. B. 1955 *Numerical Mathematical Analysis.* Baltimore, Md.: The Johns Hopkins Press.

STREET, R. L. 1963 Supercavitating flow about a slender wedge in a transverse gravity field. *J. Ship. Res.* **7**, 1, 14–23.